


## Research Article

# Site-specific serology unveils cross-reactive monoclonal antibodies targeting influenza A hemagglutinin epitopes

Philipp C. G. Pappaditis<sup>1</sup> , Alexander Fruehwirth<sup>1</sup>, Kajetana Bevc<sup>1</sup> , Jun Siong Low<sup>1</sup> , Josipa Jerak<sup>1</sup> , Laura Terzaghi<sup>1</sup>, Mathilde Foglierini<sup>1</sup> , Blanca Fernandez<sup>1</sup>, David Jarrossay<sup>1</sup>, Davide Corti<sup>3</sup> , Federica Sallusto<sup>1,2</sup> , Antonio Lanzavecchia<sup>3,4</sup>  and Antonino Cassotta<sup>1</sup> 

<sup>1</sup> Institute for Research in Biomedicine, Università della Svizzera italiana, Bellinzona, Switzerland

<sup>2</sup> Institute for Microbiology, ETH Zurich, Zurich, Switzerland

<sup>3</sup> Humabs Biomed SA, a subsidiary of Vir Biotechnology, Bellinzona, Switzerland

<sup>4</sup> National Institute of Molecular Genetics, Milano, Italy

Efficient identification of human monoclonal antibodies targeting specific antigenic sites is pivotal for advancing vaccines and immunotherapies against infectious diseases and cancer. Existing screening techniques, however, limit our ability to discover monoclonal antibodies with desired specificity. In this study, we introduce a novel method, blocking of binding (BoB) enzyme-linked immunoassay (ELISA), enabling the detection of high-avidity human antibodies directed to defined epitopes. Leveraging BoB-ELISA, we analyzed the antibody response to known epitopes of influenza A hemagglutinin (HA) in the serum of vaccinated donors. Our findings revealed that serum antibodies targeting head epitopes were immunodominant, whereas antibodies against the stem epitope, although subdominant, were highly prevalent. Extending our analysis across multiple HA strains, we examined the cross-reactive antibody response targeting the stem epitope. Importantly, employing BoB-ELISA we identified donors harboring potent heterosubtypic antibodies targeting the HA stem. B-cell clonal analysis of these donors revealed three novel, genealogically independent monoclonal antibodies with broad cross-reactivity to multiple HAs. In summary, we demonstrated that BoB-ELISA is a sensitive technique for measuring B-cell epitope immunogenicity, enabling the identification of novel monoclonal antibodies with implications for enhanced vaccine development and immunotherapies.

**Keywords:** Antibodies · Infectious diseases · Vaccination



Additional supporting information may be found online in the Supporting Information section at the end of the article.

## Introduction

**Correspondence:** Dr. Antonino Cassotta and Dr. Philipp C. G. Pappaditis  
e-mail: antonino.cassotta@irb.usi.ch; philipp.pappaditis@weizmann.ac.il

Influenza A virus is a main public health concern, causing 3.5–5 million cases of severe disease and 300,000–500,000 deaths

© 2024 Vir Biotechnology and The Author(s). *European Journal of Immunology* published by Wiley-VCH GmbH.

www.eji-journal.eu

This is an open access article under the terms of the Creative Commons Attribution-NonCommercial-NoDerivs License, which permits use and distribution in any medium, provided the original work is properly cited, the use is non-commercial and no modifications or adaptations are made.

annually, primarily in vulnerable populations [1]. In addition, the highly evolving nature of influenza viruses causes intermittent outbreaks of epidemic or pandemic proportions by transmission of novel strains from zoonotic hosts [2]. The threat of a spillover of novel influenza A viruses is persistent particularly for avian-origin highly pathogenic H5N1 and H7N9 strains that caused hundreds of severe or fatal human cases in the past decades [3], limited only by inefficient human-to-human transmission. Current measures to prevent influenza severe infections rely on whole virus-inactivated trivalent influenza vaccines (TIVs) produced in fertilized eggs. TIVs include two Influenza A strains, an H1N1 strain derivative from the 2009 pandemic, an H3N2 strain derivative from the 1968 pandemic, and one Influenza B strain, established by tracking systems of circulating seasonal strains [4]. However, TIVs need to be reformulated yearly for their strain composition, and their effectiveness is moderate, especially in immunocompromised and elderly individuals [5–9]. In recent years, also quadrivalent influenza vaccines (QIVs) have been recommended in many countries introducing a second strain of Influenza B lineage [10]. Furthermore, live-attenuated vaccines and recombinant hemagglutinin (HA) protein vaccines have also been licensed [10]. However, the low effectiveness of the currently licensed vaccines in combination with the constant threat of pandemic outbreaks from zoonotic hosts emphasizes the necessity for a universal influenza vaccine that would confer long-lasting protection, which is still a major challenge of our time.

Most influenza-neutralizing antibodies are directed to the two surface glycoproteins and in particular to HA [11], which mediates the binding of influenza virus to sialic acid on the surface of target cells. Influenza A viruses have been identified to carry 18 different HA subtypes [12] that share an amino acid sequence identity between 40% and 70% [13], categorizing them phylogenetically into group 1 or group 2 [11]. HA is a homotrimeric integral membrane protein, constituted of a variable globular head domain containing the receptor-binding motive and a more conserved, helical stem domain, which mediates the endosomal fusion of viral and cellular membranes. Five antigenic sites have been characterized for the H1 head domain: Sa, Sb, Ca1, Ca2, and Cb [14–16]. Head epitopes are targeted by potentially neutralizing antibodies, that however are primarily strain-restricted [17] and are prone to select escape mutants [14]. Stem-targeting antibodies, on the other hand, are capable of heterosubtypic cross-neutralization of several influenza A strains or even across groups [17] and are associated with potent induction of Fc-dependent immune responses [11, 18–22]. Anti-stem antibodies are classically characterized by lower neutralizing titers and have been shown to correlate with protection against influenza virus infection in humans after infection [23, 24]. However, stem-targeting antibodies are more difficult to elicit due to limited accessibility of the cognate epitope that imposes structural constraints [25]. Responses against the stem domain characterize the primary response to heterologous HAs [11, 26, 27], are associated with low pre-existing serological titers [28], and can arise from the repeated stimulation of specific memory B cells [29]. This is likely due to the recall of memory B cells bearing HA group-specific

antibodies targeting the stem, a phenomenon known as group-specific imprinting [30]. Analysis of sporadic human infections with the highly pathogenic influenza strains H5N1 and H7N9 provided strong evidence that HA group imprinting during childhood indeed can provide effective, lifelong protection against severe infection and death from viruses of the same phylogenetic group [31]. Determining the immunogenicity of head and stem antigenic sites targeted by B cells is crucial [30, 32, 33], since epitope masking by pre-existing antibodies may play an important role in modulating the reduced antibodies response to the HA stem [34]. Studies in mice and humans with H1N1 viruses have shown that the response to HA is dominated by antibodies against the antigenic sites Sa and Sb [32, 33]. However, previous studies were mainly based on hemagglutination inhibition assays as readout, thus failing in detecting antibodies incapable of hemagglutination [33], or restricting their analysis to antibodies targeting HA head, thus neglecting the stem epitopes despite their importance for cross-protection [32, 33].

Current vaccines elicit mainly antibodies targeting the HA head domain, thus not providing persistent protection to multiple influenza strains. Aiming to ensure long-lasting protection from a multitude of influenza strains, the next-generation vaccines are envisaged to target less variable viral structures such as the conserved HA stem epitope. Stem-only immunogens have been engineered to study human serological responses [35, 36], showing a wide prevalence of broadly reactive antibodies to multiple group 1 HA subtypes [37, 38]. Collectively, these studies primarily focused on cross-reactivity within group 1 HA and did not provide a direct comparison to individual head epitopes. The design of such a universal influenza vaccine has been difficult due to the lack of detailed information about key epitopes within the HA stem region driving broad immunity. Identification of broadly neutralizing antibodies (bnAbs) to all subtypes of influenza viruses offers the opportunity to analyze their binding modalities and to determine the most promising targets, thereby guiding the future design of broadly protective vaccine strategies.

To this aim, high-precision techniques are needed to screen large cohort of donors and rapidly identify donors harboring monoclonal antibodies with desired specificity, such as broadly cross-reactive antibodies. Here, we introduce a newly developed competition enzyme-linked immunosorbent assay (ELISA)-based technique that determines the antibody response to defined epitopes of interest [39] utilizing biotin-labeled reference antibodies. We called this new method blocking of binding (BoB) ELISA and optimized and standardized it for high sensitivity and low background. This robust technique introduces a novel feature that allows the conversion of dilution titers, classically used in competition ELISAs, into concentration equivalent units. The novel approach allows for a high-throughput site-specific serological analysis. We demonstrate the power of BoB-ELISA by performing a large analytical study aimed at identifying donors that elicit antibody responses of desired specificity. Analysis of the site-specific antibody response showed the immunodominance of the Sa and Sb epitopes over the stem epitopes, the latter being targeted by subdominant but highly prevalent antibodies.

In addition, heterosubtypic humoral immune response to the conserved stem epitope were shown to be induced by the vaccines in a HA group-specific manner. Additionally, BoB-ELISA allowed the identification of a donor with a potent heterosubtypic stem-specific response that was not identified by classical ELISA assays using whole recombinant HAs. Isolation of peripheral memory B cells from that donor resulted in the identification of three novel potent heterosubtypic antibodies targeting a conserved stem epitope, which were genealogically independent and did not utilize gene segments classically associated with anti-stem responses.

## Results

### Selection of an antibody panel to broadly map hemagglutinin epitopes

To establish an antibody panel that would comprehensively capture the antigenic sites characterized for the H1 head [14–16] and stem domain, we utilized H1-specific neutralizing monoclonal antibodies originating from a healthy donor that was subject of multiple previous studies of our laboratory [11, 27, 29, 40–45]. Previous studies on this donor identified antibodies of remarkable breadth [11, 29] targeting the stem epitope [46], and allowed the identification of an antibody targeting a novel epitope at the membrane-proximal external region (MPER) [43]. We utilized stem-specific (FI6, FE43) and MPER-specific (FISW84) antibodies and additional antibodies of unknown epitope specificity to perform viral escape mutant experiments. Briefly, monoclonal antibody-resistant mutants were identified by culturing the swine flu pandemic H1N1 virus with a high dose of the selected neutralizing monoclonal antibodies. The surviving viral particles carrying escape mutations were cultured under the continuous presence of the same monoclonal antibody, and the selected viral particles were sequenced to identify point mutations. The clustering of several point mutations in the same region from different selected viral particles allowed us to assign each monoclonal antibody to a specific antigenic site of HA (Fig. 1A–C; Supporting Information Fig. S1). Antibodies FISW15, FISW85, and FISW238 selected several distinct mutants in both the Sa and Sb epitope (150-loop and 190-helix, respectively) as did FISW58, a member of the recently characterized Sa/Sb-targeting multi-donor antibody class including also antibodies FISW18, FISW20 and FISW89, thus confirming crystallography analysis [42]. Antibodies FISW77 and FISW86 selected mutants in the Ca1 and Ca2 antigenic sites of HA, respectively. FISW84 selected mutants within the antigenic MPER site, confirming published cryo-EM data [43]. Importantly, stem-specific antibodies did not lead to the isolation of viral escape mutants despite several attempts, in line with the notion that single mutations cannot be easily accommodated in the stem domain of HA without compromising its function. None of the antibodies analyzed was specific for the Cb epitope, which therefore is missing from our analysis. For each of the monoclonal antibodies, we determined the half-maximal effective concentration (EC50) to H1-HA as a measurement for

their affinity (Fig. 1C, Supporting Information Fig. S2A–C). Overall, this approach allowed us to establish a panel of monoclonal antibodies targeting different HA epitopes, thus allowing a broad characterization of influenza HA epitopes targeted by human antibodies.

### BoB-ELISA enables robust screening of epitope-specific antibody response

Classical competition ELISA-based methods do not allow a quantitative analysis of epitope-specific antibody response (Fig. 2A). To overcome this limitation, we set out to develop a novel assay to map antibody response to different antigenic sites of HA in a robust and high-throughput manner. To this aim, we selected a panel of the characterized monoclonal antibodies that specifically target different HA epitopes (Fig. 1C; Supporting Information Fig. S2A–C) and used them as reference probes in the BoB-ELISA. The selected antibodies did not cross-detect other H1-HA epitopes (Supporting Information Fig. S2D). These probe antibodies were biotinylated and used to determine the epitope-specific Binding Dilution 80 (BD80) values of samples, which are determined by plotting the inhibitory signal against the dilution factor. The novelty of the BoB-ELISA relies on the conversion of the BD80 values into a concentration estimate. This is achieved by titrating a known starting concentration of the un-biotinylated antibody that is used as a reference probe, to compete with a fixed concentration (EC70) of its biotinylated isoform (Supporting Information Fig. S2E). The resulting titration curve allows the calculation of a binding concentration 80 (BC80). This BC80 value serves as an epitope-specific reference concentration, permitting the transformation of BD80 values obtained from other samples into concentration estimates. We refer to this extrapolated value as Ig concentration equivalent units (ICEU), and we used this parameter to determine the robustness, precision, and sensitivity of the newly developed BoB-ELISA assay.

To define the robustness of the assay we compared different conditions, using probe antibodies to compete with titrated samples. In the first round of tests, we compared three commonly used experimental conditions of competition ELISA; antigen-coated plates were incubated with serial dilutions of sera or unlabeled reference antibody, while subsequently labeled reference antibody was added at effective concentration (EC) 70 or EC30. Alternatively, for the third condition, the sample dilutions and labeled reference antibodies were premixed and added together to the antigen-coated plates. Using this approach, we measured very similar ICEU for the Ca2 epitope and the less accessible stem epitope, as determined in pre- and post-vaccination sera of three donors (Fig. 2B and C). Furthermore, when we used known concentrations of the unlabeled reference antibodies (FISW86 for Ca2 and FE43 for stem), ICEU values did not deviate among conditions and accurately extrapolated the correct antibody concentration that was applied in the assay (Fig. 2B and C). The low variance in the results indicates that our assay is robust across several experimental conditions and is

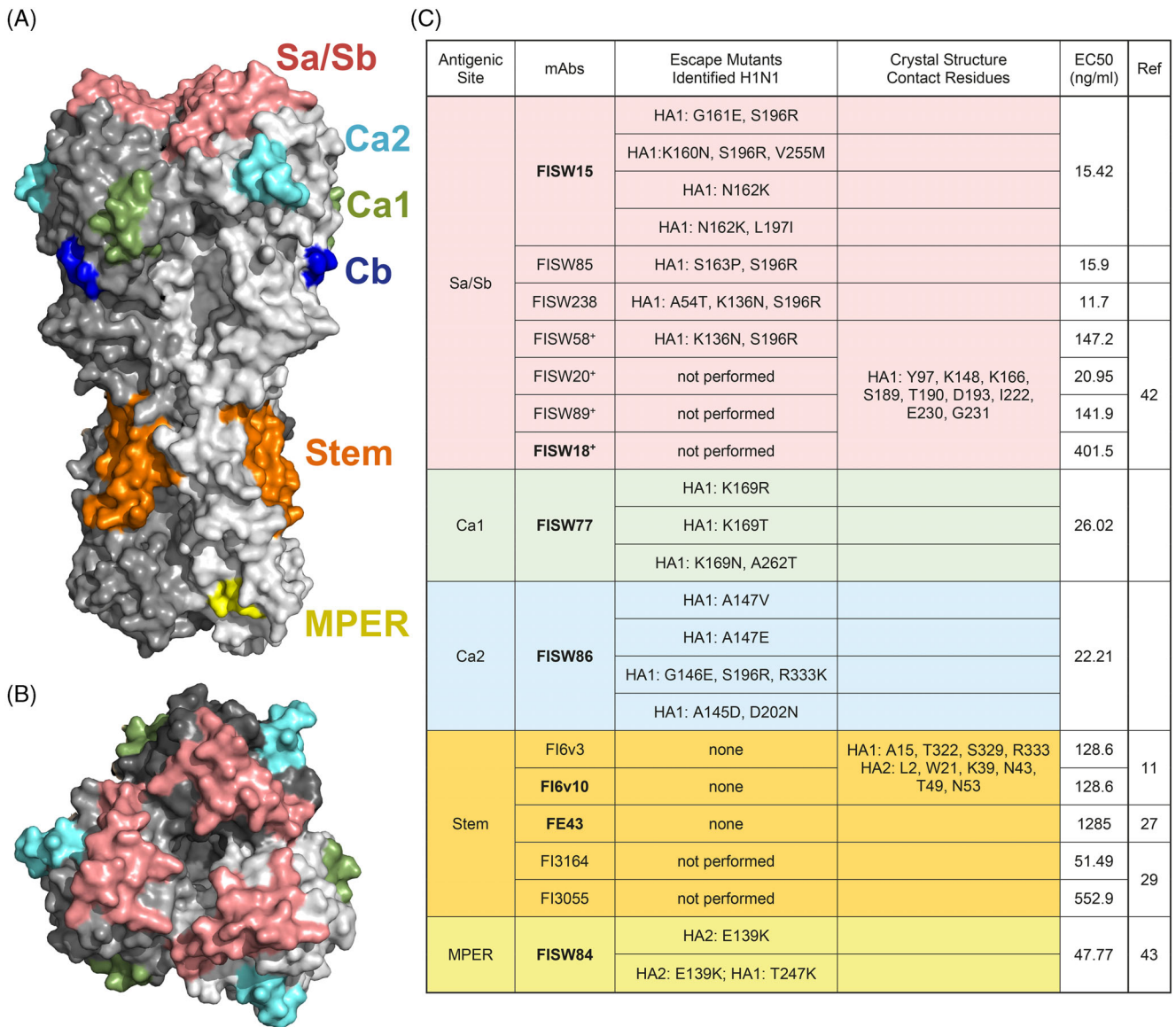


**Figure 1.** H1-HA-specific antibodies targeting divergent epitopes were selected as reference probes for the BoB-ELISA assay. (A, B) Crystallography structure in the side view (A) or top view (B) of the trimeric hemagglutinin (HA) from the H1N1 A/California/04/2009 Virus (PDB: 3UBE), represented as molecular surfaces. The antigenic sites Sa/Sb (rosa), Ca1 (green), Ca2 (blue), Cb (dark blue), Stem (orange), and MPER (yellow) are indicated. (C) Table of antigenic site specificity of characterized monoclonal antibodies. Antigenic site specificity was determined by mapping viral escape mutants, using H1-HA strain A/California/07/2009 as a reference. For each antibody, their epitope specificity, viral escape mutants, known contact residues, and EC50 values for H1-HA are indicated. Amino acid positions are indicated according to H1 numbering. Multidonor antibody class utilizing the VH2-70 gene are indicated with a “+” symbol. Monoclonal antibodies used as reference probes in the BoB-ELISA are highlighted in bold characters.

not affected by the epitope’s structural localization. Given that the different experimental conditions achieved similar precision and robustness, for the following screens we chose the addition of EC70 probe antibody to the samples as standard procedure.

Next, we addressed the effect of antibody affinities on the assay calculations for the probe antibodies as well as for the sample antibodies. To this aim, we selected two epitopes, the Sa/Sb epitope located in the accessible head domain, and the more concealed stem epitope. Specifically, for the Sa/Sb epitope we utilized both the high-affinity FISW15 (EC50 = 15 ng/mL) and the low-affinity FISW18 (EC50 = 400 ng/mL) antibodies as

reference probes. Analogously, for the stem epitope we selected as probes the high-affinity F16 (EC50 = 129 ng/mL) and the low-affinity FE43 (EC50 = 1285 ng/mL) antibodies (Supporting Information Fig. S2A). As sample antibodies, we used monoclonals targeting the same epitopes with different affinities. For the Sa/Sb epitope, we used FISW20 (EC50 = 21 ng/mL) and FISW89 (EC50 = 142 ng/mL; Supporting Information Fig. S2B), whereas for the stem epitope, FI3164 (EC50 = 52 ng/mL) and FI3055 (EC50 = 553 ng/mL) were selected (Supporting Information Fig. S2C). Sample antibodies were used alone or mixed in different ratios (3:1, 1:1, and 1:3) to obtain mixed antibody samples

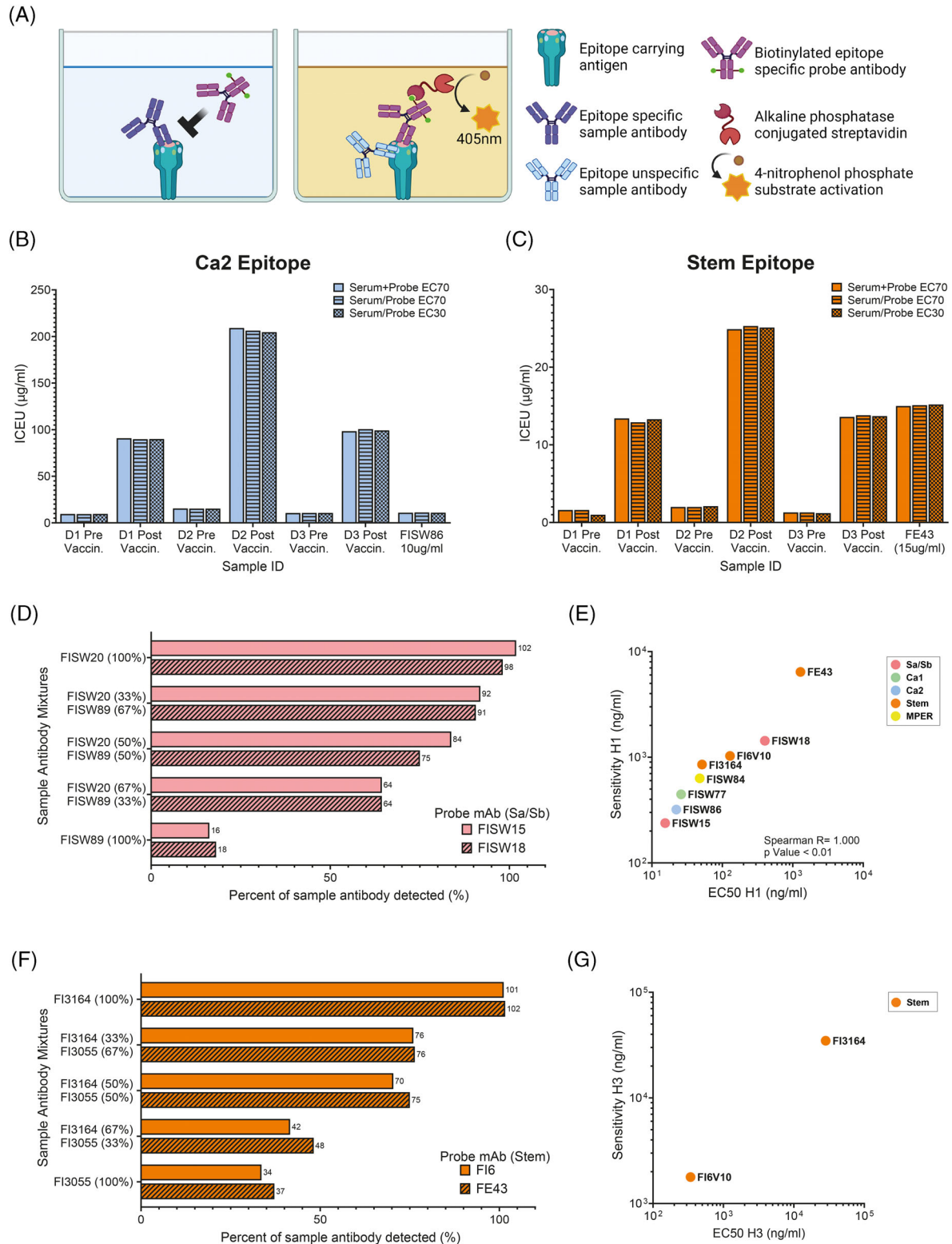


**Figure 2.** Variables affecting the detection of site-specific antibodies by BoB-ELISA. (A) Schematic representation of the BoB-ELISA assay rationale. Created with BioRender.com. (B, C) Comparison of BoB-ELISA experimental conditions. FISW86 (Ca2-specific) (B) and FE43 (stem-specific) (C) monoclonal antibodies were used to detect site-specific serum antibody levels in pre- and post-vaccination sera of three selected donors. Additional samples tested are the unlabeled probe antibodies added at 10 and 15 µg/mL, respectively. Antigen-coated plates were incubated with serial dilutions of sera or with unlabeled probe antibody and after 1 h labeled reference probe antibody was added at EC70 or EC30 concentrations for another 1 h. Alternatively, serum dilutions and labeled probes were added together (premixed samples). The serum concentration of site-specific antibodies was determined using a standard curve made with known concentrations of the unlabeled probe antibody. We refer to this value as Ig

with diverging avidities for each epitope while maintaining the total antibody concentration constant. Using either high- or low-affinity probe antibodies provided similar ICEU concentrations at all ratios used, for both the two Sa/Sb specific (Fig. 2D) and the stem-specific epitope (Fig. 2F). Together, these results indicate that the BoB-ELISA approximations are independent of the affinity of the probe antibody used. Furthermore, the assay exhibits precision when estimating concentrations of high-avidity antibodies, whereas it progressively underestimates the presence of antibodies with lower avidities.

Finally, the sensitivity of the BoB-ELISA was addressed for each probe antibody to test the lower detection limit of sample antibodies. The sensitivity for each epitope was determined as the lowest concentration of the unbiotinylated reference antibody where a BC80 could still be detected. The sensitivity of the BoB-ELISA varied amongst different probe antibodies utilized, independently of the epitopes targeted by the probe antibodies. By plotting the sensitivity of each of the probe antibodies against their EC50 value to H1-HA, we demonstrate that the detection limit of the assay is proportional to the affinity of the probe antibody utilized but independent of the epitope targeted (Fig. 2E; Supporting Information Fig. S2F). For example, FISW15 and FISW18 targeting both the Sa/Sb epitopes at different affinities varied over a 10-fold range of sensitivity (Fig. 2E). We further investigated this finding by analyzing the sensitivity of stem-targeting probe antibodies to the H3-HA strain. We took advantage of the high breadth of two stem-specific antibodies, namely FI3164 and FI6. FI3164 displays a higher affinity to H1 as compared with FI6, but a much lower affinity to H3. Correspondingly, the sensitivity to H3-HA was much higher for FI6 than FI3164 (Fig. 2G; Supporting Information Fig. S2G), thus confirming results that sensitivity is proportional to their respective antigen affinity.

Overall, these data show that the BoB-ELISA is a robust method with a wide dynamic range, high specificity, and sensitivity. Furthermore, it shows that the BoB-ELISA assay preferentially detects high-avidity antibody reducing the background of the assay to a minimum, especially important when analyzing sera frequently containing low-avidity, polyreactive antibodies.

### BoB-ELISA reveals immunodominant and subdominant antibody response to influenza HA

To determine the dynamics of induction of antibody response to each HA epitope, we used BoB-ELISA on longitudinal sera

samples obtained from the same donor from which the probe antibodies were originally isolated (Fig. 3A). Serial blood samples were collected at two weeks after antigen exposure over a period of 5 years, during which the donor was repeatedly exposed to influenza including a documented infection with the H1/California/07/09 pandemic strain in 2009. Antibodies to the HA stem were detected at all time-points at relatively constant levels, while antibodies to the MPER were present at lower levels. Conversely, antibodies to the H1/Ca09 head only appeared after booster vaccination with the matched 2010 seasonal vaccine and were detected at all next time-points although at variable and generally decreasing ICEU. These findings are consistent with the notion that antibodies to the stem region reflect a long-lived subdominant cross-reactive response, while antibodies to the head of Ca09 HA are recalled at high levels after each booster immunization [30].

To address the distribution of serum antibody responses to the antigenic sites of HA and measure their immunogenicity in a larger number of individuals, we performed site-specific serology by BoB-ELISA in a cohort of vaccinated ( $n = 175$ ) and unvaccinated ( $n = 256$ ) donors collected at steady state (Supporting Information Fig. S3A and B; Supporting Information Table S1). Cohort groups were age-matched (Supporting Information Fig. S3C) to consider the shift in dominant strain responses based on age [31]. Overall, we observed a significant increase of antibody titers targeting each of the HA epitopes in vaccinated donors as compared with unvaccinated (Fig. 3B). However, antibody titers varied greatly across donors, spanning three logs of ICEU and showed differences depending on the epitope targeted. The strongest antibody response was directed toward the head epitopes Sa/Sb, Ca1, and Ca2 that emerged as immunodominant, whereas the titers of antibodies targeting stem and MPER epitope were lower. Despite being subdominant, antibodies targeting the stem epitope were highly prevalent, since they were detected in all donors as compared with antibodies targeting other epitopes (Fig. 3B). Additionally, we observed increased titers of serum antibodies targeting the stem epitope in elderly individuals, consistent with a skewing of the antibody response that occurs with age possibly due to repeated exposures to heterosubtypic viral strains (Supporting Information Fig. S3A and B). These results indicate that the human antibody responses to the Sa/Sb, Ca1, and Ca2 epitopes located in the HA head are immunodominant, consistent with previous reports of immunodominant strain-specific antibody responses [33]. Moreover, these results demonstrate that the current influenza vaccines induce a diverse antibody response directed to several HA epitopes in most donors, including a highly prevalent anti-stem response.

concentration equivalent units (ICEU). (D, F) The assay preferentially detects high-avidity antibodies. (D) The assay was set up using Sa/Sb-specific antibody probes of high affinity (FISW15, EC50 = 15 ng/mL) or low affinity (FISW18, EC50 = 400 ng/mL). Shown are the values calculated for Sa/Sb antibodies of high affinity (FISW20, EC50 = 21 ng/mL), or low affinity (FISW89, EC50 = 142 ng/mL) tested at the known concentration of 15 µg/mL, alone or in different proportions. (F) The assay was set up using HA stem-specific antibody probes of high affinity (FI6, EC50 = 129 ng/mL) or low affinity (FE43, EC50 = 1285 ng/mL). Shown are the values calculated for stem-specific antibodies of high affinity (FE3164, EC50 = 52 ng/mL), or low affinity (FE3055, EC50 = 553 ng/mL) tested at the known concentration of 15 µg/mL, alone or in different proportions. (E, G) Correlation between EC50 values of the probe antibodies and the sensitivity of the assay. For each antibody are shown the sensitivity values against the affinity (EC50) for H1-HA (E) and H3-HA (G).

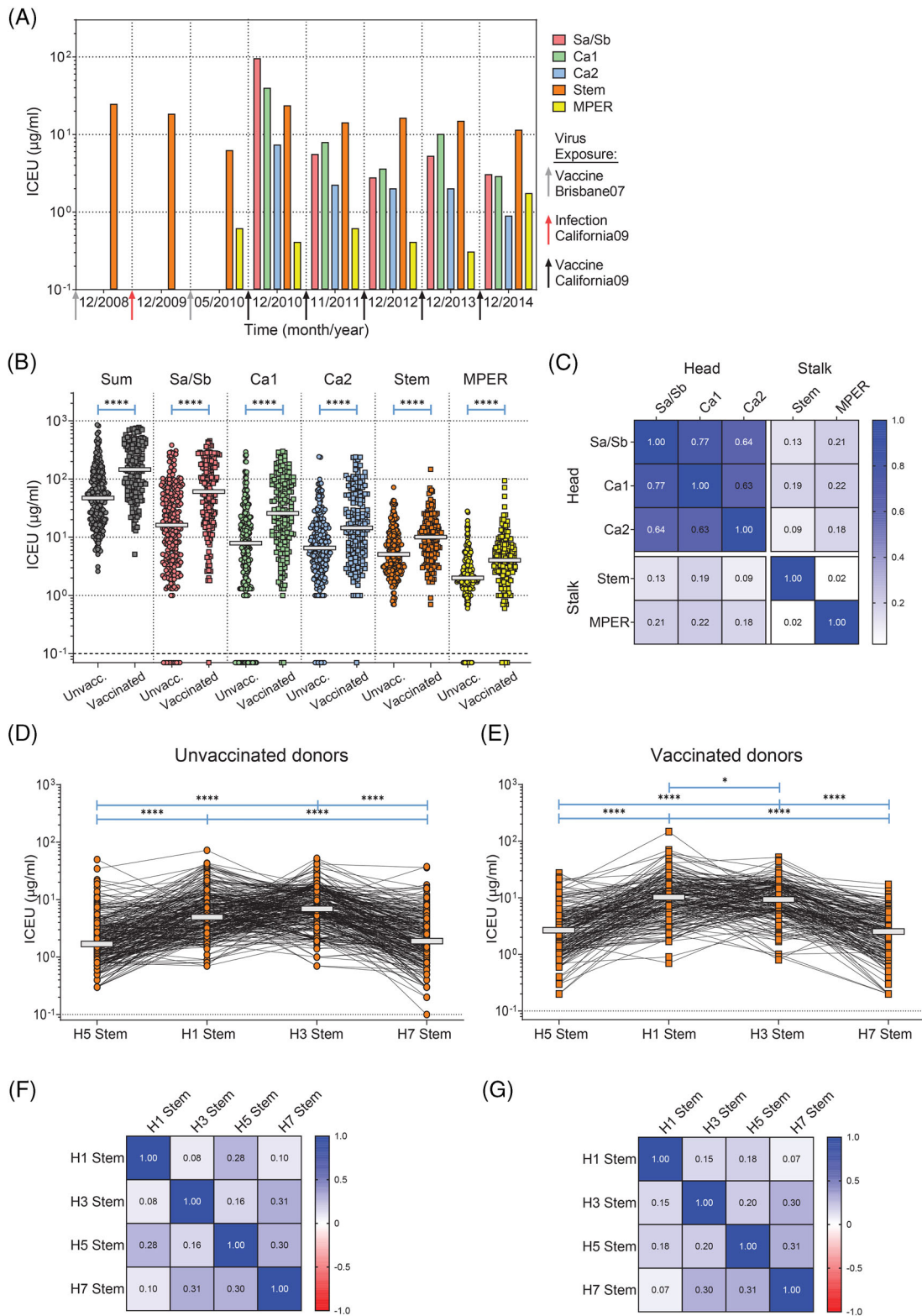


**Figure 3.** Immunodominant and subdominant serum antibodies targeting distinct HA epitopes detected by BoB-ELISA. (A) Serial blood donations of the same individual were collected over a period of 6 years and antibody response to H1-HA epitopes was analyzed via BoB-ELISA. The titers of serum antibodies targeting different sites of H1-HA are reported as color-coded bars: Sa/Sb (rosa), Ca1 (green), Ca2 (blue), Stem (orange), and MPER (yellow). At each time-point, sera were collected two weeks post influenza vaccination or infection. The H1N1 strain of the vaccine or infection of the donor is shown in gray (Vaccine Brisbane07), red (Infection California09), or black (Vaccine California09). (B) Sera of a cohort composed of age-matched unvaccinated ( $n = 256$ ) and influenza-vaccinated ( $n = 175$ ) donors analyzed via BoB-ELISA. Each dot represents the serum titer measured for each H1-HA epitope for each donor. Each H1-HA epitope is color-coded: Sa/Sb (rosa), Ca1 (green), Ca2 (blue), Stem (orange) and MPER (yellow).

To address the magnitude of antibody responses induced against each HA epitope within the same donor, we determined the Spearman correlation coefficient for each pair of epitopes. Antibody titers to the head epitopes showed a strong correlation, while anti-head and anti-stem responses poorly correlated to each other (Fig. 3C). Furthermore, donors with a strong antibody response to the stem showed no correlation with the antibody response to MPER, thus suggesting that different epitopes of the stalk domain are targeted with different propensities.

To study the cross-reactivity of antibody responses we screened the stem-specific antibody titers to the HAs of H1N1 and H3N2 influenza A strains included in the trivalent vaccine, as well as HAs of the highly pathogenic subtypes H5N1 and H7N9 that are not included in vaccines and sporadically cause severe human infections [3]. To address the titers of cross-reactive antibodies targeting the stem epitope, we took advantage of the high binding breath of FI6 [11] and performed BoB-ELISAs using FI6 as probe antibody to different HAs (Fig. 3D and E). As expected, the titers of antibodies targeting the stem of H1 and H3 (both contained in the vaccine) were significantly higher than the antibodies binding the H5 and H7 stem epitopes in both unvaccinated (Fig. 3D) and vaccinated donors (Fig. 3F). Moreover, antibody response to the stem of H1, H3, and H5 but not of H7 was significantly upregulated in vaccinated donors compared with unvaccinated donors (Supporting Information Fig. S3D). This data suggests that current H1- and H3-containing vaccines can induce a heterosubtypic antibody response to the stem of H5 but not the H7 subtype. Spearman correlation calculated pairwise for anti-stem antibodies targeting each HA subtype revealed a correlation between the HA subtype belonging to the same influenza group, that is, H1 and H5 (group 1) and H3 and H7 (group 2; Fig. 3F and G; Supporting Information Fig. S3E–J). Interestingly, we also observed an equally strong correlation between H5- and H7-targeting antibodies, despite belonging to different influenza groups.

To investigate the neutralizing properties of tested sera, we performed microneutralization assays [42, 44] that showed a significant upregulation of neutralizing antibody titers (inhibitory dilution; ID50) in vaccinated donors (Supporting Information Fig. S4A). To determine which site-specific antibodies were contributing to the protective abilities of the sera, we correlated the neutralization titers ID50 with antibody ICEUs for each HA epitope (Supporting Information Fig. S4B and C). Sera-neutralizing titers correlated strongly with the anti-head antibody responses in both vaccinated and unvaccinated donors, but not with antibody responses targeting the stem or MPER epitopes (Supporting Information Fig. S4C). This data indicates that head-specific antibodies are the major source of neutralization as measured *in vitro*

and that antibodies targeting different HA epitopes are contributing to neutralization in a proportional manner in both vaccinated and unvaccinated donors.

Collectively our data show that individuals receiving currently licensed vaccines have higher antibody titers targeting all HA epitopes, particularly the HA head epitopes that emerge as immunodominant. Conversely, the HA stem is targeted by subdominant but highly prevalent antibodies that show group-specific correlation and heterosubtypic responses, raising the question of whether vaccination induced these antibodies.

### Influenza vaccination induces subdominant heterosubtypic anti-stem antibodies

To dissect how pre-existing antibodies elicited by previous influenza exposures can affect the induction and boosting of antibodies targeting different HA sites upon new exposure to the antigen, we sought to follow the serologic responses before and 4 weeks after booster vaccination. Serum samples of 26 adult donors (Supporting Information Fig. S5A and B, Supporting Information Table S2) were analyzed via BoB-ELISA, while simultaneous micro-neutralization assays were performed on the same sera. The results showed a significant increase in antibody titers after vaccination for all HA epitopes (Fig. 4A). However, each donor showed an individual pattern of site-specific responses to the vaccine (Supporting Information Fig. S5A), with in general a marked response to the head epitopes. Neutralization assays revealed a strong increase in neutralization titers upon vaccination that was proportional to pre-existing neutralizing titers (Supporting Information Fig. S5C and D). Head epitopes yielded much stronger antibody titers upon immunization when compared with stem epitopes (Fig. 4A). Spearman coefficient calculated for each epitope-specific response before and after vaccination showed a strong correlation for head epitopes but not for the stem and MPER epitopes (Fig. 4B). This indicates that induction of head-specific responses upon vaccination is proportional to the pre-existing titers against those epitopes, something not observed for stem and MPER epitopes. Of note, after vaccination the levels of antibodies targeting the head, but not the stem or MPER, showed a good correlation with neutralizing titers (Supporting Information Fig. S5E–H).

To dissect the antibody response to influenza vaccination at the clonal level, we isolated peripheral blood IgG<sup>+</sup> memory B cells *ex vivo* at 4 weeks after immunization and generated Epstein–Barr virus (EBV)-immortalized B-cell clones [47]. The culture supernatants of HA-specific B-cell clones were tested by BoB-ELISA to

← Epitope summation is shown in gray. Median values are reported as grey lines. \* $p \leq 0.05$ , \*\* $p \leq 0.01$ , \*\*\* $p \leq 0.001$ , \*\*\*\* $p \leq 0.0001$  as determined by two-tailed unpaired t-test. (C) Heatmap reporting the Spearman R correlation index calculated for each pair of epitopes in the head and stalk domain of H1-HA.  $N = 431$  donors (pool of unvaccinated and vaccinated). (D, E) Serum samples were analyzed for their reactivity to H1, H3, H5, and H7 stem epitopes using the monoclonal FI6 as probe antibody. Titers of serum antibodies targeting each of the four HA analyzed are shown for each unvaccinated ( $n = 256$ ) (D) and vaccinated ( $n = 175$ ) (E) donor. Median values are reported as grey lines. \* $p \leq 0.05$ , \*\* $p \leq 0.01$ , \*\*\* $p \leq 0.001$ , \*\*\*\* $p \leq 0.0001$  as determined by two-tailed paired t-test. (F, G) Heatmaps of the pairwise Spearman R correlation index of stem-specific antibodies are shown for unvaccinated (F) and vaccinated (G) donors.



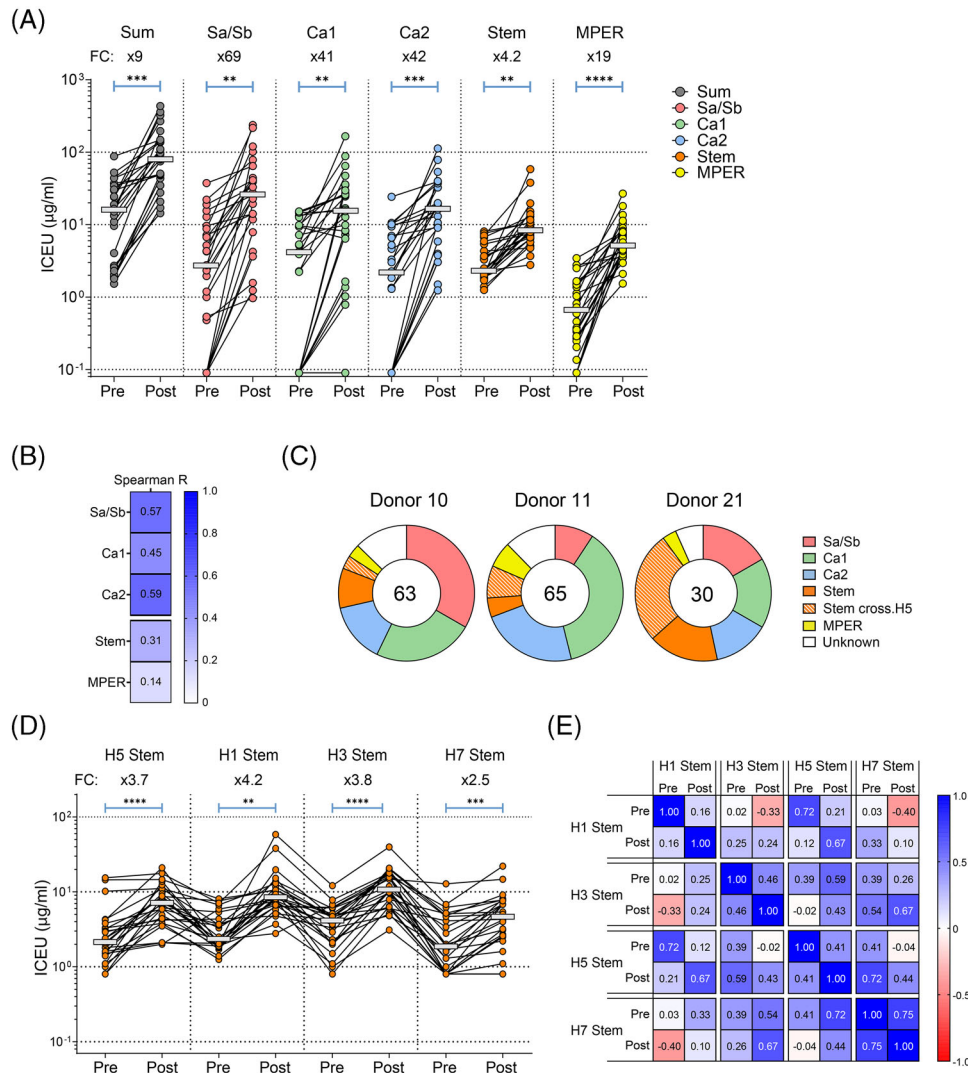


**Figure 4.** Induction of heterosubtypic antibodies by influenza vaccination. (A) Serum samples were collected from adult donors ( $n = 26$ ) before and four weeks after influenza vaccination. The titers of H1-HA site-specific antibodies in sera collected before and after immunization were determined by BoB-ELISA. Each dot represents the serum titer measured for each H1-HA epitope for each donor. Each H1-HA epitope is color-coded: Sa/Sb (rosa), Ca1 (green), Ca2 (blue), Stem (orange) and MPER (yellow). Epitope summation (FC) of the antibody titers is reported for each epitope. Median values are reported as grey lines.  $*p \leq 0.05$ ,  $**p \leq 0.01$ ,  $***p \leq 0.001$ ,  $****p \leq 0.0001$  as determined by two-tailed paired t-test. (B) Spearman R index of correlation between antibody titers in pre- and post-vaccination sera is reported for each H1-HA epitope. (C) EBV-immortalized B-cell clones were generated from IgG<sup>+</sup> memory B cells isolated *ex vivo* from the PBMCs of three high-responder vaccinated individuals four weeks after influenza vaccination. The culture supernatants of HA-specific B-cell clones were tested by BoB-ELISA to determine the epitope specificity of each antibody-secreting B-cell clone. The pie charts report the distribution of B-cell clones specific for each H1-HA epitope. Slices in the charts represent different H1-HA epitopes and their size is proportional to the number of B-cell clones targeting the same epitope. The total number of clones analyzed is reported at the center of the pie chart. The culture supernatants of H1 stem-specific clones were further analyzed for binding to H5-HA by ELISA, and cross-reactive clones were reported with a diagonal fill pattern. (D) Titers of serum antibodies targeting the stem epitope of H5-HA, H1-HA, H3-HA, and H7-HA were measured by BoB-ELISA before and after vaccination. The mean fold change (FC) of the antibody titers is reported for each epitope. Median values are reported as grey lines.  $*p \leq 0.05$ ,  $**p \leq 0.01$ ,  $***p \leq 0.001$ ,  $****p \leq 0.0001$  as determined by two-tailed paired t-test. (E) Heatmap of the pairwise Spearman R correlation index between antibody titers targeting the stem of H5-HA, H1-HA, H3-HA, and H7-HA measured in the serum collected before and after vaccination.

determine the epitope specificity of each antibody-secreting B-cell clone. Clonal analysis of three high-responder vaccinated individuals revealed a broad response with B-cell clones targeting all HA epitopes, including several stem-specific clones that cross-reacted with H5-HA (Fig. 4C). Collectively, these findings indicate that after vaccination the serum antibody response by plasma cell burst is mirrored by a diverse repertoire of circulating IgG<sup>+</sup> mem-

ory B cells targeting different HA epitopes, in line with our previous findings [40].

To determine if current vaccines can induce stem-specific antibody responses of heterosubtypic nature, we used BoB-ELISA assays on the sera collected before and after immunization to measure their antibody titers to the stem epitopes of H1, H3, H5, and H7 influenza HA strains described previously. Vaccination of

donors resulted in a significant increase of antibodies directed to the stem from all HA strains analyzed (Fig. 4D). However, antibodies targeting the H7 stem showed the lowest fold change after vaccination, suggesting that the induction of heterosubtypic antibodies against H7 by currently licensed vaccines is challenging [17]. Analysis of Spearman R values showed a good overall correlation between the serum titers of anti-stem antibodies targeting multiple HA strains (Fig. 4E), suggesting the induction of cross-reactive antibodies.

Collectively, these findings demonstrate that current influenza vaccines induce both strain-specific antibodies targeting the head epitopes, and cross-reactive antibodies targeting the stem. Despite being highly personalized in each donor analyzed, the antibody response induced by vaccination shows in general a dominance towards the HA head, while anti-stem antibodies cross-reactive to multiple HA strains remain subdominant.

### BoB-ELISA facilitates the isolation of broadly cross-reactive monoclonal antibodies

Previous studies showed that during the course of an immune response broadly reactive, stem-specific antibodies can be elicited [11, 27, 29]. We sought to utilize the BoB-ELISA technique as a tool to identify donors that elicited potent broadly cross-reactive antibodies, due to its efficiency in detecting high-avidity antibodies. To this aim, we performed pairwise comparisons of the stem-specific antibodies measured by BoB-ELISA in the serum of the post-vaccination cohort ( $n = 26$ ). Specifically, we compared pairwise the antibody titers targeting the stem of H1 and H3 HAs (Fig. 5A), or H5 and H7 HAs (Fig. 5B), that are contained or not in the currently licensed vaccines, respectively. As a reference, we used a serum sample from Donor FI6 collected in December 2010 (Fig. 3A), when the bnAb FI6 was originally isolated [11]. With this approach, we found that the serum of Donor 21 contained high titers of antibodies targeting the stem of all HAs tested at a similar level to the serum of Donor FI6. This suggested the presence of broadly cross-reactive stem-specific monoclonal antibodies and a high frequency of circulating memory B cells targeting the HA stem. Interestingly, classical ELISA screens using whole recombinant HAs performed on sera of the same cohort did not distinguish Donor 21 (Supporting Information Fig. S6A), thus highlighting the sensitivity of the BoB-ELISA technique in detecting site-specific high-avidity serum antibodies.

To confirm the serology data at the clonal level and to isolate broadly cross-reactive monoclonal antibodies, EBV-immortalized B-cell clones were generated from peripheral blood IgG<sup>+</sup> memory B cells from Donor 21 and screened via classic ELISA against the H1, H3, H5, and H7 HAs (Fig. 5C and D). The screening revealed the presence of many B-cell clones producing monoclonal antibodies capable of broad heterosubtypic binding to multiple HAs of the same and even different phylogenetic groups. Secondary ELISA screens of selected B-cell clones revealed three potent broadly binding antibodies, namely ADCF06, ADCF101, and ADCF148 that were sequenced (Fig. 5E) and expressed

as recombinant monoclonal antibodies [48]. Sequence analysis of immunoglobulin genes revealed three different VH gene segments, which were not previously associated with stem-specific heterosubtypic antibodies. Phylogenetic trees from the antibodies of interest were generated using Ancestry [49] and their related unmutated common ancestor (UCA) was determined, revealing that these antibodies originated from genealogically unrelated UCAs (Supporting Information Fig. S6B). Titration curves revealed higher affinity of ADCF06, ADCF101, and ADCF148 monoclonals to most HAs tested as compared with their respective UCAs, thus proving that these antibodies are affinity matured (Fig. 5F–K). Nevertheless, the mutated monoclonal antibodies showed a range of affinities to HAs of different subtypes (Fig. 5F–H; Supporting Information Fig. S6B and C), with ADCF101 showing high affinity to influenza B HA and being able to cross-react to multiple influenza A HAs. Indeed, the genealogical reconstruction revealed distinct developmental pathways of these three heterosubtypic antibodies (Supporting Information Fig. S6B). ADCF06 originated from UCA1 which weakly binds to H3-HA. The extensive affinity maturation of ADCF06 with 34 somatic mutations in the H chain and 18 in the L chain indicates a prolonged and complex somatic hypermutation process, resulting in increased antibody affinity and breadth. The antibody ADCF101 originated from UCA2 with an affinity only for influenza type B HA and through somatic mutations acquired breadth to influenza type A HAs while simultaneously increasing affinity to HA of influenza type B. The ADCF148 antibody originated from UCA3 showing binding to H5 and H7 HAs, that subsequently through somatic mutations increased in breadth to the H1 and H3 HA strains encountered by vaccination, while in parallel, increasing affinity to H5 and H7 HAs that are antigens the donor was likely not exposed to. Together, these results show that multiple BCR gene segment rearrangements and affinity maturation pathways can occur in parallel in the same individual, resulting in the generation of heterosubtypic broadly binding antibodies.

Overall, we showed that screening site-specific serum antibodies by BoB-ELISA allows identifying donors with strong heterosubtypic antibody responses and carrying a high frequency of circulating memory B cells targeting the HA stem. BoB-ELISA coupled with B-cell clonal analysis allowed us to characterize three novel stem-targeting antibodies that broadly reacted to multiple HA strains and developed through three distinct pathways of affinity maturation. Overall, these findings highlight the potency of BoB-ELISA screens to identify donors carrying antibodies of desired specificity.

## Discussion

To facilitate the isolation of human monoclonal antibodies targeting antigenic sites of interest we designed, optimized, and standardized a new competition ELISA that allows the deconvolution of the humoral immune responses in large-scale screens. BoB-ELISA allowed the preferential detection of high-avidity antibodies in contrast to low-avidity antibodies. This feature enabled

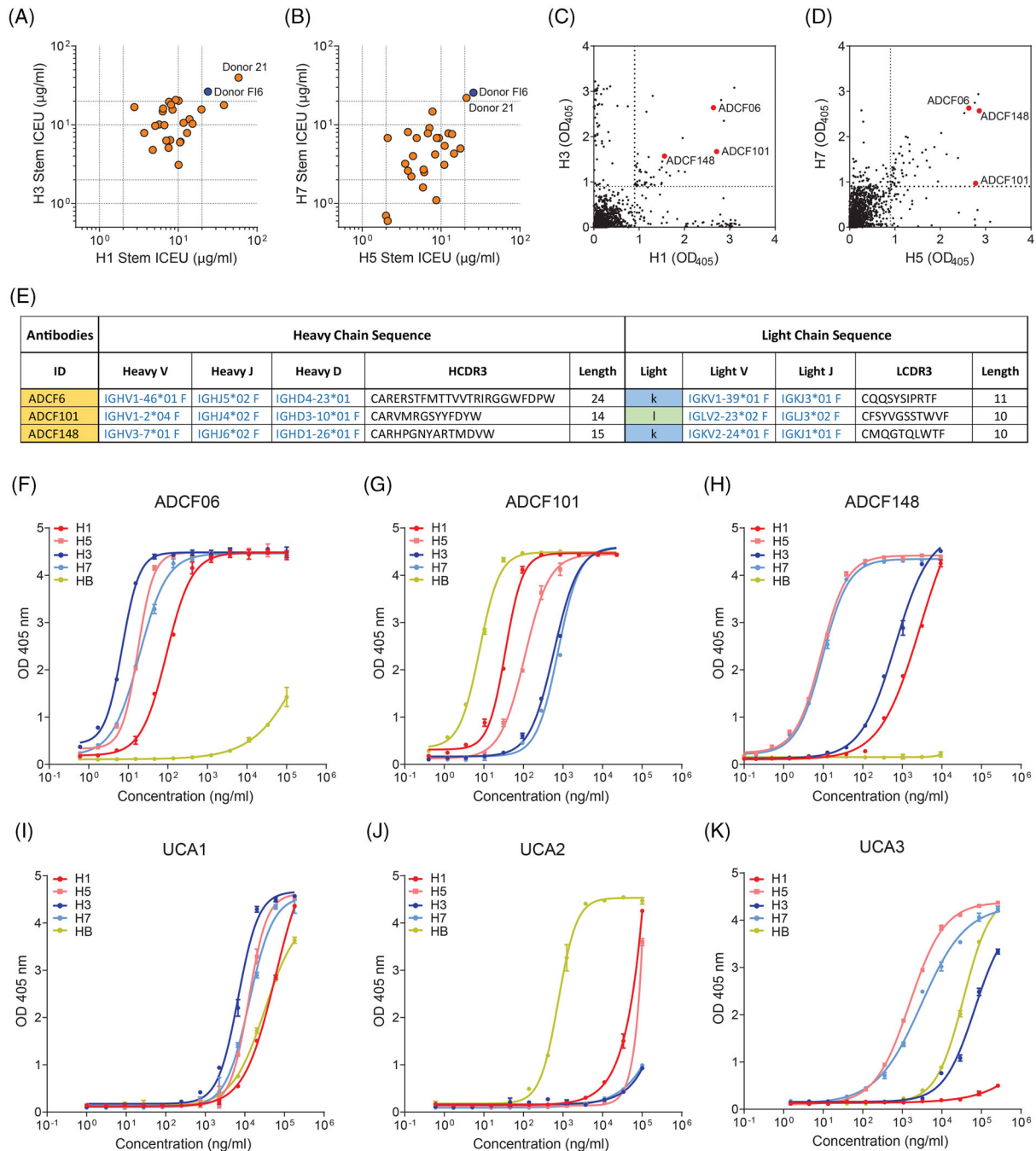


**Figure 5.** BoB-ELISA screening facilitates the isolation of broadly cross-reactive antibodies. (A, B) Titers of serum antibodies targeting the stem epitope of H1, H3, H5, and H7 HAs were measured by BoB-ELISA on sera collected from adult donors ( $n = 27$ ) after influenza vaccination. The titers of antibodies targeting the stem of H1-HA and H3-HA (A), or the stem of H5-HA and H7-HA (B) are shown as scatter plots. Each dot represents a donor. The response in the donor from which the broadly cross-reactive F16 monoclonal antibody was isolated (Donor F16) is shown in blue. Highlighted is the response in Donor 21. (C, D) EBV-immortalized B-cell clones were generated from IgG<sup>+</sup> memory B cells isolated *ex vivo* from the peripheral blood mononuclear cells (PBMCs) of Donor 21. Culture supernatants ( $n = 11'520$  wells) were screened for the presence of HA-specific IgG antibodies by classic ELISA using H1, H3, H5, and H7 recombinant HAs. Shown is the scatter plot of the reactivity of each individual B-cell clone to H1-HA and H3-HA (C), or H5-HA and H7-HA (D). Each dot represents the optical density (OD) values at 405 nm of individual culture supernatants tested for each recombinant HA, after subtraction of OD values obtained from PBS-coated plates. Dotted lines indicate the thresholds for specificity. Three B-cell clones producing IgG antibodies potentially reacting against group 1 and group 2 HAs are highlighted as red dots (ADCF06, ADCF101, and ADCF148), and were confirmed by subsequent secondary ELISA assays. (E) Sequence analysis of the three novel broadly cross-reactive monoclonal antibodies identified in (D). V(D)J gene usage and CDR3 sequence for the H and L chains were determined using the IMGT database. (F–K) Antibodies reported in (E) and their unmutated common ancestors (UCAs) were produced as recombinant monoclonal antibodies. UCAs were generated using the Ancestree software. Recombinant monoclonal antibodies were tested for their binding affinity to various HAs from influenza A (H1, H3, H5, and H7) and influenza B (HB) by classic ELISA. The titration curves of binding are shown for monoclonal antibodies ADCF06 (F), ADCF101 (G), and ADCF148 (H), as well as their respective UCAs, namely UCA1 (I), UCA2 (J), and UCA3 (K).

a semiquantitative estimation of site-specific antibody responses. The preferential detection of high-avidity antibodies allowed minimizing the background of the assay filtering out low-avidity antibodies, ensuring that the detected values represent a minimal yet site-specific response. This aspect is beneficial when analyzing sera frequently containing low-avidity, polyreactive antibodies. Furthermore, BoB-ELISA allows the estimation of the collective serum antibody titers of all isotypes simultaneously with a remarkably high sensitivity. We utilized the BoB-ELISA to study the antibody response induced by the influenza vaccine on a large cohort of donors, and we extrapolated the distribution of antibodies targeting the HA epitopes in the highly variable head domain and the more conserved stem domain. By analyzing the serum responses of the donor from whom we isolated the probe antibodies, we characterized a stem-specific response that was persistently detected over multiple years. These results contribute to our previous findings that showed by mass spectrometry-based serum analysis [50, 51] that the humoral response to influenza is dominated by a small number of persistent antibodies targeting the HA stem [44], thus confirming the accuracy of the BoB-ELISA.

Focusing on the H1N1 strain that caused the 2009 pandemic, we demonstrated that donors induce an antibody response against several epitopes of the head and the stem domains. We identified Sa and Sb epitopes in the HA head as immunodominant antigenic sites, in accordance with previous studies performed in mice and humans [32, 33]. Despite being subdominant, stem-targeting antibody titers were identified above the sensitivity threshold consistently in all donors analyzed. These results suggest that stem-targeting antibodies can be induced by vaccination or previous viral infections but remain subdominant, maybe due to low structural accessibility of the cognate epitope. Furthermore, stem-directed antibody responses induced by currently licensed vaccines generated antibodies of heterosubtypic nature, being able to target also viral antigens from related influenza strains that are not included in the vaccine. These antibodies cross-reacted to HAs of group 1 and 2, in a HA-group-specific manner, also for group 2-specific antibodies that are expected to be less frequent [17]. However, stem-specific antibody responses in vaccinated donors only poorly correlated with serum neutralization titers in contrast to infection cases as shown by recent studies [23, 24].

Screening hundreds of memory B-cell clones, we isolated and characterized three novel, potent heterosubtypic antibodies originating from independent genealogical trees. These antibodies showed broad cross-reactivity to the HA subtypes we have tested, with one of them binding even the phylogenetically distant influenza B HA. Screening of the same donor utilizing the antigen-specific memory B-cell repertoire analysis method developed in our laboratory [40] which we ameliorated recently [52] resulted in the isolation of the same heterosubtypic clones. This finding allows the speculation that these three potent heterosubtypic IgG<sup>+</sup> memory B-cell clones may be clonally expanded and present at high frequency in the blood, as we previously showed for the FI6 antibody [11].

Several studies identified stem-targeting bnAbs, describing the genetic requirements that contributed to their development.

Preferential gene segment usage and sequence signatures were characterized [11, 20, 28, 29, 41, 53, 54]. The VH1-69 gene was determined as the major contributor of potent heterosubtypic stem-targeting antibodies [27, 29, 54-57]. Alternatively, antibodies with H chains encoded by diverging gene segments have been described [27, 29, 41, 58-61], of which several contain a VH3-30 [62-64] including FI6. The combined effort of these studies strongly suggests that the stem-targeting antibody response is dominated but not restricted to a few VH gene segments [17, 25, 65]. Our work discloses the identification of three genealogically independent monoclonal antibodies that show broad binding to multiple HAs and do not utilize VH gene segments classically associated with the anti-stem response. However, antibodies targeting the stem epitope using the described gene segments have previously been reported by our laboratory [29]. These results show that multiple BCR gene segment rearrangements and parallel pathways of affinity maturation are used for the generation of heterosubtypic broadly binding antibodies, even within the same donor.

Large-scale screening of human donors by classic ELISA using recombinant antigens is usually a crucial step that precedes the isolation of potent monoclonal antibodies. Once the candidate donors are identified, the epitope specificity is determined by competition ELISAs [29, 60, 62]. Here, we report a reverse approach, where BoB-ELISA primary screening allows the direct identification of donors of interest for the isolation of monoclonal antibodies of desired epitope specificity. We propose that the preferential detection of high-avidity antibodies by the BoB-ELISA provides a sensitive approach to detect donors of interest. Indeed, using BoB-ELISA screening of a cohort of just 26 donors we successfully identified donors carrying rare stem-specific broadly cross-reactive antibodies, while the classic ELISA assay using whole recombinant HAs on the same cohort failed to discriminate these donors of interest. Therefore, the here-described technique can be utilized to complement existing techniques such as stem-only probes [35, 36], to identify stem-specific antibodies.

Taken together, our work provides a novel approach to capture the antibody response to distinct influenza HA epitopes, which could be useful for the isolation of bnAbs. Importantly, the approach here described can be easily repurposed for the identification of potent antibodies targeting emerging influenza variants as well as a wide variety of complex antigens from other pathogens. Collectively, our approach can enable large-scale screenings to isolate monoclonal antibodies of desired specificity, which may inform the development of new vaccines and the design of novel immunotherapies for the treatment of infectious diseases and cancer.

## Materials and methods

### Study subjects

Blood samples were collected from two independent cohorts of individuals. The first cohort comprised vaccinated ( $n = 175$ ) and

unvaccinated ( $n = 256$ ) individuals collected at steady state (Supporting Information Table S1) and was obtained in the framework of the Swiss Immune Setpoint Study sponsored by the Swiss Vaccine Research Institute. The second cohort comprised individuals ( $n = 26$ ) collected before and 4 weeks after vaccination with FLUarix Tetra 2015/16 (GlaxoSmithKline; Table S2) and was obtained from the Surrey Clinical Research Centre (University of Surrey). Blood from healthy donors was obtained from the Swiss Blood Donation Center of Basel and Lugano. Serial blood donations from a healthy donor who underwent annual Influenza vaccination were obtained after written informed consent. The study was approved by the Ethical Committee of Cantone Ticino, Switzerland (ref. 2018–02166/CE 3428), and by the London-Surrey Borders Research Ethics Committee (reference 15/LO/1649), and registered on ClinicalTrials.gov (reference NCT02557802). All blood donors provided written informed consent for participation in the study. Human primary cell protocols were approved by the Federal Office of Public Health (no. A000197/2 to F.S.).

### Isolation of human monoclonal antibodies

Fresh or cryopreserved peripheral blood mononuclear cells (PBMCs) were surface stained with anti-CD22-FITC (BD Pharmingen) as well as anti-IgG-APC (Jackson ImmunoResearch) and enriched via anti-FITC microbeads (Miltenyi Biotec). CD22<sup>+</sup>IgG<sup>+</sup> memory B cells were sorted by fluorescence-activated cell sorting and immortalized with EBV, CpG 2006 and cultured at limiting dilutions on irradiated allogeneic PBMCs as previously described [47]. Supernatants of immortalized and expanded memory B cells were screened after 14 days in antigen ELISA assays for specific binding to antigens of interest. Positive cultures were expanded in a complete RPMI medium for further studies and characterizations. VH and VL sequences from positive cultures were also retrieved via reverse transcriptase PCR and subsequent PCR and where required into expression vectors shown in detail in the following paragraph. In parallel VH and VL sequences were sent for sequencing to Microsynth AG, Switzerland. If necessary, purifications of antibodies were performed with protein A chromatography (GE Healthcare) and desalted against PBS (Thermo Scientific).

### Monoclonal antibody production

Selected sequences obtained by PCR (RT-PCR) and subsequent PCR of immortalized B cells were cloned into human IgG1 and Ig $\kappa$  or Ig $\lambda$  expression vectors as described previously [48]. Vectors were kindly provided by M. Nussenzweig at Rockefeller University. Monoclonal antibodies were produced by transient transfection of 293F cells (Invitrogen) using PEI in serum-free media. Cell supernatants were collected 4–8 days after transfection, filtered, and preserved by the addition of 0.1% BSA in PBS. The antibodies were affinity purified by protein A chromatography (GE Healthcare) and desalted against PBS (Thermo Scientific).

### Antibody variants generation

Germline sequences of the isolated antibodies were determined with reference to the IMGT database [66]. Antibody variants in which single or multiple germline mutations were reverted to the germline by Ancestry software [49] and produced either by synthesis (Genscript) or by site-directed mutagenesis (Promega) and confirmed by sequencing. Already published antibody sequences were obtained through the Protein Data Bank and the corresponding genes were synthesized and expressed by transient transfection. Obtained sequenced plasmids were used to produce monoclonal antibodies as described in the previous paragraph.

### Antibody biotinylation

Antibodies of interest were biotinylated using the EZ-Link NHS-PEO solid phase biotinylation kit (Thermo Scientific, cat. no. 21450) following the manufacturer's instructions. Briefly, nickel-chelated (Ni-NTA) agarose resin columns are used to first immobilize purified IgG antibodies. Antibodies are bound to the column via a nickel interaction with the histidine-rich cluster on the Fc region at the junctures of the C $\gamma$ 2 and C $\gamma$ 3 antibody domains, which is highly conserved across all mammalian IgGs. The immobilized antibodies are then biotinylated by adding a solution containing NHS-PEG4-Biotin molecules. This results in a binding of approximately 3–5 biotin molecules per antibody molecule. The agarose columns are washed to remove excess biotin, and consequently the antibody is eluted by adding a high concentration imidazole buffer.

### Structural analysis

The PDB database file 3UBE was used as a basis to visualize the HA molecule of H1N1/California/04/2009 with the PyMOL software ([www.pymol.org](http://www.pymol.org)). Antigenic site specificity of monoclonal antibodies was determined by mapping viral escape mutants, using H1-HA strain A/California/07/2009 as a reference. H1 numbering was performed using Librator [67].

### Enzyme-linked immunosorbent assay

Half-area ELISA plates (Corning) or Spectraplate-384 with high protein binding treatment (custom made from Perkin Elmer) were coated with 1 or 3  $\mu$ g/mL of recombinant protein H1 (A/H1/California/07/2009), H3 (A/Perth/16/2009), H5 (A/bar-headed goose/Qinghai/1A/2005), H7 (A/Netherlands/219/2003), or HB (B/Brisbane/60/2008) in PBS overnight at 4°C. Plates were subsequently blocked for 1 h with 1% BSA (Sigma) in PBS at room temperature. Quadruplicates of threefold serial dilutions of antibodies were incubated for 1 h at room temperature and stained, after four times washing, with an anti-total IgG-alkaline peroxidase antibody (Southern Biotechnologies).

Plates were developed after an additional quadruple washing step by adding 40  $\mu\text{L}$  p-NPP substrate (Sigma) and reading them after 30 min or 1 h at room temperature without light at 405 nm. Washing steps with PBS containing 0.05% Tween-20. Binding affinities were determined by extrapolating the concentration at which the antibody reaches 50% of the maximum signal (EC50) via four-parameter nonlinear regression with a variable slope.

### Blocking of binding ELISA

Biotinylated antibodies of interest were used at a concentration of 70% maximum OD (EC70) for each of the reference antibodies and each antigen which was determined by ELISA as previously described. Half-area ELISA plates (Corning) were coated with 1 or 3  $\mu\text{g}/\text{mL}$  of H1 (A/H1/California/07/2009), H3 (A/Perth/16/2009), H5 (A/bar-headed goose/Qinghai/1A/2005) or H7 (A/Netherlands/219/2003) (Sino Biological) recombinant protein in PBS overnight at 4°C. Plates were subsequently blocked for 1 hour with 1% BSA (Sigma) in PBS at room temperature. Samples were threefold serially diluted and then added on plates coated with the antigen of interest. After 1 h of incubation, the biotinylated antibody was added at the determined EC70 concentration and incubated for an additional hour. After quadruple washing and staining the plates for 1 h with a Streptavidin-AP conjugate (Jackson ImmunoResearch) a p-NPP substrate (Sigma) was added for 1 h and read at 405 nm. Washing steps were performed with PBS containing 0.05% Tween-20. Relative competition level of samples was determined with multiple controls without a primary sample (ODpos ctr) and multiple controls without a primary sample as well as a biotinylated antibody (ODneg ctr). The percentage of inhibition was calculated by the formula:  $(1 - (\text{OD sample} - \text{OD neg ctr}) / (\text{OD pos ctr} - \text{OD neg ctr})) \times 100$ . Absolute Ig concentrations against a specific antigenic site were transformed by using the unlabeled reference antibody of each of the biotinylated reference antibodies as a standard curve made of known concentration (CON). The values termed ICEUs were extrapolated by using the formula:

$$\text{BD80serum} \times \text{CONreference} / \text{BD80reference}.$$

### H1N1 virus microneutralization assay

Micro-neutralization assay was performed as previously reported [29, 42, 44], using the Neuraminidase activity to represent virus replication. Briefly,  $2 \times 10^7$  Madin-Darby canine kidney (MDCK) cells were cultured in T175 culture flasks (Thermo Scientific) with MEM expansion medium. The flasks were washed with PBS as well as MEM infection-medium and cells were detached by trypsin treatment. Detached cells were seeded into 96-well U-bottom plates at  $10^5$  cells/well. *In vitro* viral neutralization assays were performed by preincubating threefold serial dilution of antibody supernatant or sera with 2000 TCID50/mL of A/H1N1/California/07/2009 virus for 1 h at 37°C and then used to infect 96-well seeded MDCK cells, in MEM infection medium

(MEM + Glutamax + Eagle Salts, Kanamycin 1%, TPCK-treated Trypsin 2  $\mu\text{g}/\text{mL}$ ; Gibco). Readout was performed after a 3-days of incubation in a CO<sub>2</sub> incubator at 37°C. Culture supernatants were transferred to black opaque 96-well plates (Perkin Elmer) and a fluorescently labeled substrate (2'-(4-methylumbelliferyl)-alpha-D-N-acetylneuraminic acid sodium salt hydrate (Sigma)) was added. After 1 h of incubation at 37°C, the viral replication represented by Neuraminidase activity was quantified with an Envision Fluorometer (PerkinElmer) at EX 355 nm/EM 460 nm. The neutralization values were expressed as the antibody/serum titers that reduced the fluorescence signal by 50% (50% inhibitory dilution [ID50]) compared with virus-only control wells. The ID50 values were calculated by interpolation of neutralization curves fitted with a four-parameter nonlinear regression with a variable slope. All antibodies/sera were tested in quadruplicates.

### Isolation of viral escape mutants

Escape mutants were isolated by preincubating 10–30  $\mu\text{g}/\text{mL}$  antibody supernatant for the antibody to be characterized for epitope specificity with 10,000 TCID50/mL pandemic wild-type H1N1 A/California/07/2009 virus. The premixed antibody/virus supernatant was used to infect MDCK cells in multiple wells of a 96-well culture plate for 4 h as described for the micro-neutralization assay. After the washing steps the infected cells were cultured in infection-medium (MEM + Glutamax + Eagle Salts, Kanamycin 1%, TPCK-treated Trypsin 2  $\mu\text{g}/\text{mL}$ ; Gibco) containing a concentration of 0.5–1  $\mu\text{g}/\text{mL}$  of the same antibody of interest for constant evolutionary pressure. The cytopathic effect of each well was evaluated after 3 to 4 days of incubation at 5% CO<sub>2</sub> and 37°C. The supernatant of wells showing cytopathic effects were harvested for a subsequent infection round, as described above, and cultures that were confirmed in the secondary infection assay were further validated by performing micro-neutralization assays with the isolated variants described above. The selected viral variants that incorporated escape mutations were used for RNA isolation with a viral RNA isolation kit (Qiagen). The RNA was reverse transcribed (Omniscript RT, Qiagen) (primer: 5'-AGC RAA AGC AGG-3') and the HA sequence retrieved by PCR amplification (PCR PlatinumTaq Kit, Invitrogen) (primers: HA Cal 07/09 forward: 5'-CGC AAA TGC AGA CAC ATT A-3'; HA Cal 07/09 reverse: 5'-AGA CCC ATT AGA GCA CAT C-3'). PCR product was Sanger sequenced (Microsynth AG) using an HA-specific primer (HA Cal 07/09 forward-1: 5'-CGC AAA TGC AGA CAC ATT A-3'; HA Cal 07/09 forward-2: 5'-GGA AAT TCA TAC CCA AAG CTC AGC AAA-3'; HA Cal 07/09 reverse: 5'-AGA CCC ATT AGA GCA CAT C-3').

### Statistical analysis

All statistical analyses were performed using GraphPad Prism (V9) and Microsoft Excel of Windows 10 software. Statistical differences were analyzed with the unpaired *t*-test or one-way ANOVA was used; *p* values of 0.05 or less were considered significant.

Nonparametric Kruskal–Wallis test was used to perform multiple comparisons between the groups analyzed. Nonparametric Spearman or Pearson *R* values were calculated for statistical comparisons between pairs of data. ED50, EC50, ID50, and BD80 values were determined by nonlinear regression analysis (log(agonist) versus response (four parameters). Alignments were done with QIAGEN CLC Main Workbench, visualized via a graphic user interface in concert with the IMG2 database. All data is shown as mean  $\pm$  SEM. Mean fold change was calculated by dividing for each donor the ICEU in post-vaccination sera by the pre-vaccination ICEU, followed by the averaging of these values across all donors.

**Acknowledgements:** The authors thank all study participants and all personnel at the hospitals who donated blood and devoted time to our research. The authors also thank Diego Morone for cell sorting, Sandra Jovic, Isabella Giacchetto-Sasselli, and Chiara Silacci for technical assistance, M. Nussenzweig and H. Warde-mann for providing reagents for antibody cloning and expression, and the Swiss Vaccine Research Institute (SVRI) for providing samples.

Open access funding provided by Universita della Svizzera italiana.

**Funding information:** This study has been carried out with financial support from the European Research Council (grant no. 885539 ENGRAB to A.L.), the Swiss National Science Foundation (grant no. 176165 to A.L.), and the Commission of the European Communities, Seventh Framework Programme, contract HEALTH-2011-280873 “Advanced Immunization Technologies” (ADITEC). F.S. and the Institute for Research in Biomedicine are supported by the Helmut Horten Foundation. The funders had no role in the study design, data collection and analysis, decision to publish, or preparation of the manuscript.

**Conflict of interest:** The authors declare no financial or commercial conflict of interest.

**Author contributions:** Philipp C. G. Paparoditis, Alexander Fruehwirth, Kajetana Bevc, Jun Siong Low, Josipa Jerak, Blanca Fernandez, and Antonino Cassotta contributed to experimental work. David Jarrossay performed cell sorting. Mathilde Foglierini performed bioinformatic analyses. Philipp C. G. Paparoditis, Davide Corti, Federica Sallusto, and Antonio Lanzavecchia contributed to the study concept and experiment design. Davide Corti, Federica Sallusto, and Antonio Lanzavecchia provided supervision. Antonio Lanzavecchia and Federica Sallusto acquired the funding. Philipp C. G. Paparoditis, Antonino Cassotta, Federica Sallusto, and Antonio Lanzavecchia analyzed the data and wrote the manuscript. All authors contributed to the interpretation of data and critical revision of the manuscript.

**Data availability statement:** The data presented in this manuscript are included in the paper and the Supplementary Information. All further relevant source data that support the findings of this study are available from the corresponding authors upon reasonable request.

## References

- (WHO), W.H.O. Influenza (Seasonal). Bulletin of the World Health Organization. 2023; Available from: [https://www.who.int/news-room/factsheets/detail/influenza-\(seasonal\)](https://www.who.int/news-room/factsheets/detail/influenza-(seasonal)).
- Belshe, R. B., The origins of pandemic influenza—lessons from the 1918 virus. *N. Engl. J. Med.* 2005. 353(21): 2209–2211.
- Qin, Y., Horby, P. W., Tsang, T. K., Chen, E., Gao, L., Ou, J., Nguyen, T. H., et al. Differences in the Epidemiology of Human Cases of Avian Influenza A(H7N9) and A(H5N1) Viruses Infection. *Clin. Infect. Dis.* 2015. 61(4): 563–571.
- Kim, H., Webster, R. G. and Webby, R. J., Influenza Virus: Dealing with a Drifting and Shifting Pathogen. *Viral. Immunol.* 2018. 31(2): 174–183.
- Wei, C.-J., Crank, M. C., Shiver, J., Graham, B. S., Mascola, J. R. and Nabel, G. J., Next-generation influenza vaccines: opportunities and challenges. *Nat. Rev. Drug Discov.* 2020. 19(4): 239–252.
- Prevention, C. D. C., Past seasons vaccine effectiveness estimates. *Vaccine Effect. Stud.* 2024; Available from: <https://www.cdc.gov/flu/vaccines-work/past-seasons-estimates.html>.
- Jackson, M. L., Chung, J. R., Jackson, L. A., Phillips, C. H., Benoit, J., Monto, A. S., Martin, E. T., et al. Influenza vaccine effectiveness in the United States during the 2015–2016 season. *N. Engl. J. Med.* 2017. 377(6): 534–543.
- Beyer, W. E. P., Mcelhaney, J., Smith, D. J., Monto, A. S., Nguyen-Van-Tam, J. S. and Osterhaus, A. D. M. E., Cochrane re-arranged: support for policies to vaccinate elderly people against influenza. *Vaccine* 2013. 31(50): 6030–6033.
- Ohmit, S. E., Petrie, J. G., Malosh, R. E., Cowling, B. J., Thompson, M. G., Shay, D. K. and Monto, A. S., Influenza vaccine effectiveness in the community and the household. *Clin. Infect. Dis.* 2013. 56(10): 1363–1369.
- Chen, J.-R., Liu, Y.-M., Tseng, Y.-C. and Ma, C., Better influenza vaccines: an industry perspective. *J. Biomed. Sci.* 2020. 27(1): 33.
- Corti, D., Voss, J., Gamblin, S. J., Codoni, G., Macagno, A., Jarrossay, D., Vachieri, S. G., et al. A neutralizing antibody selected from plasma cells that binds to group 1 and group 2 influenza A hemagglutinins. *Science* 2011. 333(6044): 850–856.
- Tong, S., Zhu, X., Li, Y., Shi, M., Zhang, J., Bourgeois, M., Yang, H., et al. New world bats harbor diverse influenza A viruses. *PLoS Pathog.* 2013. 9(10): e1003657.
- Nobusawa, E., Aoyama, T., Kato, H., Suzuki, Y., Tateno, Y. and Nakajima, K., Comparison of complete amino acid sequences and receptor-binding properties among 13 serotypes of hemagglutinins of influenza A viruses. *Virology* 1991. 182(2): 475–485.
- Caton, A. J., Brownlee, G. G., Yewdell, J. W. and Gerhard, W., The antigenic structure of the influenza virus A/PR/8/34 hemagglutinin (H1 subtype). *Cell* 1982. 31(2 Pt 1): 417–427.
- Wiley, D. C., Wilson, I. A. and Skehel, J. J., Structural identification of the antibody-binding sites of Hong Kong influenza haemagglutinin and their involvement in antigenic variation. *Nature* 1981. 289(5796): 373–378.
- Gerhard, W., Yewdell, J., Frankel, M. E. and Webster, R., Antigenic structure of influenza virus haemagglutinin defined by hybridoma antibodies. *Nature* 1981. 290(5808): 713–717.

- 17 Corti, D., Camerini, E., Guarino, B., Kallewaard, N. L., Zhu, Q. and Lanzavecchia, A., Tackling influenza with broadly neutralizing antibodies. *Curr. Opin. Virol.* 2017. **24**: 60–69.
- 18 Terajima, M., Cruz, J., Co, M. D. T., Lee, J.-H., Kaur, K., Wilson, P. C. and Ennis, F. A., Complement-dependent lysis of influenza A virus-infected cells by broadly cross-reactive human monoclonal antibodies. *J. Virol.* 2011. **85**(24): 13463–13467.
- 19 Dilillo, D. J., Tan, G. S., Palese, P. and Ravetch, J. V., Broadly neutralizing hemagglutinin stalk-specific antibodies require FcγR interactions for protection against influenza virus in vivo. *Nat. Med.* 2014. **20**(2): 143–151.
- 20 Henry Dunand, C. J., Leon, P. E., Huang, M., Choi, A., Chromikova, V., Ho, I. Y., Tan, G. S., et al. Both neutralizing and non-neutralizing human H7N9 influenza vaccine-induced monoclonal antibodies confer protection. *Cell Host Microbe.* 2016. **19**(6): 800–813.
- 21 Dilillo, D. J., Palese, P., Wilson, P. C. and Ravetch, J. V., Broadly neutralizing anti-influenza antibodies require Fc receptor engagement for in vivo protection. *J. Clin. Invest.* 2016. **126**(2): 605–610.
- 22 Morgan, S. B., Holzer, B., Hemmink, J. D., Salguero, F. J., Schwartz, J. C., Agatic, G., Camerini, E., et al. Therapeutic administration of broadly neutralizing F16 antibody reveals lack of interaction between human IgG1 and FcγR receptors. *Front Immunol.* 2018. **9**: 865.
- 23 Ng, S., Nachbagauer, R., Balmaseda, A., Stadlbauer, D., Ojeda, S., Patel, M., Rajabathor, A., et al. Novel correlates of protection against pandemic H1N1 influenza A virus infection. *Nat. Med.* 2019. **25**(6): 962–967.
- 24 Aydllo, T., Escalera, A., Strohmeier, S., Aslam, S., Sanchez-Cespedes, J., Ayllon, J., Roca-Oporto, C., et al. Pre-existing Hemagglutinin Stalk antibodies correlate with protection of lower respiratory symptoms in flu-infected transplant patients. *Cell Rep. Med.* 2020. **1**(8): 100130.
- 25 Corti, D. and Lanzavecchia, A., Broadly neutralizing antiviral antibodies. *Annu. Rev. Immunol.* 2013. **31**: 705–742.
- 26 Wrammert, J., Koutsonanos, D., Li, G.-M., Edupuganti, S., Sui, J., Morrissey, M., Mccausland, M., et al. Broadly cross-reactive antibodies dominate the human B cell response against 2009 pandemic H1N1 influenza virus infection. *J. Exp. Med.* 2011. **208**(1): 181–193.
- 27 Corti, D., Suguitan, A. L., Pinna, D., Silacci, C., Fernandez-Rodriguez, B. M., Vanzetta, F., Santos, C., et al. Heterosubtypic neutralizing antibodies are produced by individuals immunized with a seasonal influenza vaccine. *J. Clin. Invest.* 2010. **120**(5): 1663–1673.
- 28 Andrews, S. F., Huang, Y., Kaur, K., Popova, L. I., Ho, I. Y., Pauli, N. T., Dunand, C. J. H., et al. Immune history profoundly affects broadly protective B cell responses to influenza. *Sci. Transl. Med.* 2015. **7**(316): 316ra192.
- 29 Pappas, L., Foglierini, M., Piccoli, L., Kallewaard, N. L., Turrini, F., Silacci, C., Fernandez-Rodriguez, B., et al. Rapid development of broadly influenza neutralizing antibodies through redundant mutations. *Nature* 2014. **516**(7531): 418–422.
- 30 Krammer, F., The human antibody response to influenza A virus infection and vaccination. *Nat. Rev. Immunol.* 2019. **19**(6): 383–397.
- 31 Gostic, K. M., Ambrose, M., Worobey, M. and Lloyd-Smith, J. O., Potent protection against H5N1 and H7N9 influenza via childhood hemagglutinin imprinting. *Science* 2016. **354**(6313): 722–726.
- 32 Angeletti, D., Gibbs, J. S., Angel, M., Kosik, I., Hickman, H. D., Frank, G. M., Das, S. R., et al. Defining B cell immunodominance to viruses. *Nat. Immunol.* 2017. **18**(4): 456–463.
- 33 Liu, S. T. H., Behzadi, M. A., Sun, W., Freyn, A. W., Liu, W.-C., Broecker, F., Albrecht, R. A., et al. Antigenic sites in influenza H1 hemagglutinin display species-specific immunodominance. *J. Clin. Invest.* 2018. **128**(11): 4992–4996.
- 34 Zarnitsyna, V. I., Ellebedy, A. H., Davis, C., Jacob, J., Ahmed, R. and Antia, R., Masking of antigenic epitopes by antibodies shapes the humoral immune response to influenza. *Philos. Trans. R. Soc. Lond. B. Biol. Sci.* 2015. **370**(1676): 20140248.
- 35 Yassine, H. M., Boyington, J. C., Mctamney, P. M., Wei, C.-J., Kanekiyo, M., Kong, W.-P., Gallagher, J. R., et al. Hemagglutinin-stem nanoparticles generate heterosubtypic influenza protection. *Nat. Med.* 2015. **21**(9): 1065–1070.
- 36 Impagliazzo, A., Milder, F., Kuipers, H., Wagner, M. V., Zhu, X., Hoffman, R. M. B., Van Meersbergen, R., et al. A stable trimeric influenza hemagglutinin stem as a broadly protective immunogen. *Science* 2015. **349**(6254): 1301–1306.
- 37 Yassine, H. M., Mctamney, P. M., Boyington, J. C., Ruckwardt, T. J., Crank, M. C., Smatti, M. K., Ledgerwood, J. E., et al. Use of Hemagglutinin stem probes demonstrate prevalence of broadly reactive group 1 influenza antibodies in human sera. *Sci. Rep.* 2018. **8**(1): 8628.
- 38 Smatti, M. K., Nasrallah, G. K., Al Thani, A. A. and Yassine, H. M., Measuring influenza hemagglutinin (HA) stem-specific antibody-dependent cellular cytotoxicity (ADCC) in human sera using novel stabilized stem nanoparticle probes. *Vaccine* 2020. **38**(4): 815–821.
- 39 Wang, M. L., Skehel, J. J. and Wiley, D. C., Comparative analyses of the specificities of anti-influenza hemagglutinin antibodies in human sera. *J. Virol.* 1986. **57**(1): 124–128.
- 40 Pinna, D., Corti, D., Jarrossay, D., Sallusto, F. and Lanzavecchia, A., Clonal dissection of the human memory B-cell repertoire following infection and vaccination. *Eur. J. Immunol.* 2009. **39**(5): 1260–1270.
- 41 Kallewaard, N. L., Corti, D., Collins, P. J., Neu, U., McAuliffe, J. M., Benjamin, E., Wachter-Rosati, L., et al. Structure and function analysis of an antibody recognizing all influenza A subtypes. *Cell* 2016. **166**(3): 596–608.
- 42 Cheung, C. S.-F., Fruehwirth, A., Paparoditis, P. C. G., Shen, C.-H., Foglierini, M., Joyce, M. G., Leung, K., et al. Identification and structure of a multi-donor class of head-directed influenza-neutralizing antibodies reveal the mechanism for its recurrent elicitation. *Cell Rep.* 2020. **32**(9): 108088.
- 43 Benton, D. J., Nans, A., Calder, L. J., Turner, J., Neu, U., Lin, Y. P., et al. Influenza hemagglutinin membrane anchor. *Proc. Natl. Acad. Sci. USA* 2018. **115**(40): 10112–10117.
- 44 Lee, J., Paparoditis, P., Horton, A. P., Fruehwirth, A., Mcdaniel, J. R., Jung, J., Boutz, D. R., et al. Persistent antibody clonotypes dominate the serum response to influenza over multiple years and repeated vaccinations. *Cell Host Microbe.* 2019. **25**(3): 367–376.e5.
- 45 Cassotta, A., Paparoditis, P., Geiger, R., Mettu, R. R., Landry, S. J., Donati, A., Benevento, M., et al., Deciphering and predicting CD4+ T cell immunodominance of influenza virus hemagglutinin. *J. Exp. Med.* 2020. **217**(10): e20200206.
- 46 Okuno, Y., Isegawa, Y., Sasao, F. and Ueda, S., A common neutralizing epitope conserved between the hemagglutinins of influenza A virus H1 and H2 strains. *J. Virol.* 1993. **67**(5): 2552–2558.
- 47 Traggiai, E., Becker, S., Subbarao, K., Kolesnikova, L., Uematsu, Y., Gismondo, M. R., Murphy, B. R., et al. An efficient method to make human monoclonal antibodies from memory B cells: potent neutralization of SARS coronavirus. *Nat. Med.* 2004. **10**(8): 871–875.
- 48 Tiller, T., Meffre, E., Yurasov, S., Tsuiji, M., Nussenzweig, M. C. and Wardemann, H., Efficient generation of monoclonal antibodies from single human B cells by single cell RT-PCR and expression vector cloning. *J. Immunol. Methods* 2008. **329**(1-2): 112–124.
- 49 Foglierini, M., Pappas, L., Lanzavecchia, A., Corti, D. and Perez, L., Ancestree: an interactive immunoglobulin lineage tree visualizer. *PLoS Comput. Biol.* 2020. **16**(7): e1007731.



- 50 Lavinder, J. J., Wine, Y., Giesecke, C., Ippolito, G. C., Horton, A. P., Lungu, O. I., Hoi, K. H., et al. Identification and characterization of the constituent human serum antibodies elicited by vaccination. *Proc. Natl. Acad. Sci. USA* 2014. **111**(6): 2259–2264.
- 51 Lavinder, J. J., Horton, A. P., Georgiou, G. and Ippolito, G. C., Next-generation sequencing and protein mass spectrometry for the comprehensive analysis of human cellular and serum antibody repertoires. *Curr. Opin. Chem. Biol.* 2015. **24**: 112–120.
- 52 Low, J. S., Jerak, J., Tortorici, M. A., Mccallum, M., Pinto, D., Cassotta, A., Foglierini, M., et al. ACE2-binding exposes the SARS-CoV-2 fusion peptide to broadly neutralizing coronavirus antibodies. *Science* 2022. **377**(6607): 735–742.
- 53 Lingwood, D., Mctamney, P. M., Yassine, H. M., Whittle, J. R. R., Guo, X., Boyington, J. C., Wei, C.-J., et al. Structural and genetic basis for development of broadly neutralizing influenza antibodies. *Nature* 2012. **489**(7417): 566–570.
- 54 Lang, S., Xie, J., Zhu, X., Wu, N. C., Lerner, R. A. and Wilson, I. A., Antibody 27F3 broadly targets influenza A group 1 and 2 Hemagglutinins through a further variation in V(H)1-69 antibody orientation on the HA stem. *Cell Rep.* 2017. **20**(12): 2935–2943.
- 55 Throsby, M., Van Den Brink, E., Jongeneelen, M., Poon, L. L. M., Alard, P., Cornelissen, L., Bakker, A., et al. Heterosubtypic neutralizing monoclonal antibodies cross-protective against H5N1 and H1N1 recovered from human IgM+ memory B cells. *PLoS One* 2008. **3**(12): e3942.
- 56 Sui, J., Hwang, W. C., Perez, S., Wei, G., Aird, D., Chen, L.-M., Santelli, E., et al. Structural and functional bases for broad-spectrum neutralization of avian and human influenza A viruses. *Nat. Struct. Mol. Biol.* 2009. **16**(3): 265–273.
- 57 Dreyfus, C., Laursen, N. S., Kwaks, T., Zuijgeest, D., Khayat, R., Ekiert, D. C., Lee, J. H., et al. Highly conserved protective epitopes on influenza B viruses. *Science* 2012. **337**(6100): 1343–1348.
- 58 Joyce, M. G., Wheatley, A. K., Thomas, P. V., Chuang, G.-Y., Soto, C., Bailer, R. T., Druz, A., et al. Vaccine-induced antibodies that neutralize group 1 and group 2 influenza A viruses. *Cell* 2016. **166**(3): 609–623.
- 59 Wu, Y., Cho, M., Shore, D., Song, M., Choi, J., Jiang, T., Deng, Y.-Q., et al. A potent broad-spectrum protective human monoclonal antibody crosslinking two haemagglutinin monomers of influenza A virus. *Nat. Commun.* 2015. **6**: 7708.
- 60 Li, G.-M., Chiu, C., Wrammert, J., Mccausland, M., Andrews, S. F., Zheng, N.-Y., Lee, J.-H., et al. Pandemic H1N1 influenza vaccine induces a recall response in humans that favors broadly cross-reactive memory B cells. *Proc. Natl. Acad. Sci. USA* 2012. **109**(23): 9047–9052.
- 61 Ekiert, D. C., Friesen, R. H. E., Bhabha, G., Kwaks, T., Jongeneelen, M., Yu, W., Ophorst, C., et al. A highly conserved neutralizing epitope on group 2 influenza A viruses. *Science* 2011. **333**(6044): 843–850.
- 62 Nakamura, G., Chai, N., Park, S., Chiang, N., Lin, Z., Chiu, H., Fong, R., et al. An in vivo human-plasmablast enrichment technique allows rapid identification of therapeutic influenza A antibodies. *Cell Host. Microbe* 2013. **14**(1): 93–103.
- 63 Tharakaraman, K., Subramanian, V., Viswanathan, K., Sloan, S., Yen, H.-L., Barnard, D. L., Leung, Y. H. C., et al. A broadly neutralizing human monoclonal antibody is effective against H7N9. *Proc. Natl. Acad. Sci. USA* 2015. **112**(35): 10890–10895.
- 64 Wyrzucki, A., Dreyfus, C., Köhler, I., Steck, M., Wilson, I. A. and Hangartner, L., Alternative recognition of the conserved stem epitope in influenza A virus hemagglutinin by a VH3-30-encoded heterosubtypic antibody. *J. Virol.* 2014. **88**(12): 7083–7092.
- 65 Li, Y., Wang, L., Si, H., Yu, Z., Tian, S., Xiang, R., Deng, X., et al. Influenza virus glycoprotein-reactive human monoclonal antibodies. *Microbes Infect.* 2020. **22**(6-7): 263–271.
- 66 Lefranc, M.-P., IMGT, the International ImMunoGeneTics Information System. *Cold Spring Harb. Protoc.* 2011. **2011**(6): 595–603.
- 67 Li, L., Changrob, S., Fu, Y., Stovicek, O., Guthmiller, J. J., McGrath, J. J. C., Dugan, H. L., et al. Librator: a platform for the optimized analysis, design, and expression of mutable influenza viral antigens. *Brief Bioinform.* 2022. **23**(2): bbac028.

**Abbreviations:** **BD80:** Binding Dilution 80 · **bnAbs:** broadly neutralizing antibodies · **BoB:** blocking of binding · **EBV:** Epstein-Barr virus · **EC:** effective concentration · **ELISA:** enzyme-linked immunosorbent assay · **HA:** hemagglutinin · **ICEU:** Ig concentration equivalent units · **MDCK:** Madin-Darby canine kidney cells · **MPER:** membrane-proximal external region · **PBMCs:** peripheral blood mononuclear cells · **QIVs:** quadrivalent influenza vaccines · **TIVs:** trivalent influenza vaccines · **UCA:** unmutated common ancestor

**Full correspondence:** Dr. Antonino Cassotta and Dr. Philipp C. G. Paparoditis, Institute for Research in Biomedicine, Università della Svizzera Italiana, 6500 Bellinzona, Switzerland  
e-mail: antonino.cassotta@irb.usi.ch;  
philipp.paparoditis@weizmann.ac.il

**Present address:** Philipp C. G. Paparoditis, Department of Systems Immunology, Weizmann Institute of Science, 7610001, Rehovot, Israel.

Received: 1/2/2024

Revised: 3/7/2024

Accepted: 5/7/2024

Accepted article online: 8/7/2024